SUPPLEMENATL FIGURE LEGENDS

Fig. S1. ***A (inset box),*** The Complex I isolated from bovine heart contains up to 45 different subunits as analyzed by SDS-PAGE using 4-12% Bis-tris gel (*MWM denotes molecular weight marker*). ***B,*** *Out of these 45 subunits, there are 14 highly conserved core subunits in the complex I from different species. There are 7 core subunits in the hydrophobic subcomplex.* Based on the known protein crystal structures of the core subunits from *T. thermophilus* (**hydrophilic domain, PDB ID: 3I9V**) *and E. coli* (**hydrophobic subcomplex, PDB ID: 3RKO**), we have produced a model scheme showing the locations of 51 kDa and 75 kDa subunits in the core functional Complex I. 51 kDa subunit (in light cyan color) and 75 kDa subunit (in light green color) reside at the top of the core hydrophilic domain, which contains FMN cofactor (magentas sticks model) and iron-sulfur clusters (orange-yellow spheres model), and hosts the initial step of respiratory electron transfer activities.

Fig. S2. Amino acid sequence of the precursor of the complex I-75 kDa subunit. The regions labeled with bold represent the amino acid residues identified with LC/MS/MS under the non-reduced conditions in the absence of β-ME. The cysteinyl residues involved in S-glutathionylation are highlighted with gray and they are C_{226}, C_{367}, and C_{727}. The cysteinyl residues involved in disulfide linkage are C_{554}, *and* C_{564}. The region labeled with a dotted underline is the N-terminal extension (aa 1-23), which acts as an import sequence and does not exist in the mature protein.

Fig. S3. MS/MS spectra of the protonated molecular ions of S-glutathionylated peptides (*a*) $_{361}$VDADTLC^{367}TEEVFPTAGAGTDLR$_{382}$, and (*b*) $_{713}$AVTEGAHAVEEPSIC^{727}.

Fig. S4. Effect of complex I-mediated $O_2^{\bullet-}$ generation on the ratio of GSH/GSSG (*in A)* and the enzymatic activity of complex I (*in B*) under the conditions of enzyme turnover in the presence of GSH. The reaction mixture is as described in the legend of the Figure 1. The concentrations of GSH/GSSG and the enzymatic activity of complex I were measured after 1 h incubation at 37^{o} C.

Fig. S5. Amino acid sequence of the precursor of the complex I-75 kDa subunit. The regions labeled with bold represent the amino acid residues identified with LC/MS/MS under the reduced conditions in the presence of β-ME. The cysteinyl residues involved in protein radical formation are underlined and they are C_{226}, C_{554}, *and* C_{727}. The region labeled with a dotted underline is the N-terminal extension (aa 1-23), which acts as an import sequence and does not exist in the mature protein.

Fig. S6. MS/MS spectrum of the triply protonated molecular ion of DMPO-binding peptide $_{544}$MLFLLGADGGC^{554}ITR$_{557}$.

Fig. S7. MS/MS spectra of the doubly protonated molecular ions of S-sulfonated peptides. *a,* $_{713}$AVTEGAHAVEEPSIC(SO$_3$)^{727}. *b,* $_{544}$M(ox)LFLLGADGGC^{554}(SO$_3$)ITR$_{557}$.

Fig. S8. The homology model of 75 kDa (pale green) subunit of Complex I. FMN (magentas sticks) and iron-sulfur clusters (orange-yellow spheres) are also shown for orientation. There are total 17 highly conserved cysteines in mature mammal 75 kDa subunits. According to our multiple sequence alignment results (data not shown), 11 of the 17 cysteines are identical to the Nqo3 subunit of *T. thermophilus*, and directly involved in the coordinates or ligands of the iron-sulfur clusters, and they are highlighted with magentas sticks. The other 6 cysteines (C_{53}, C_{367}, C_{554}, C_{564}, C_{710} and C_{727}) are labeled and highlighted in blue-yellow spheres. Except C_{53}, all other five active cysteines are surface exposed according to the homology model.

Fig. S9. The effect of different dosages of menadione (0-100 μM) on the HL-1 cellular S-glutathionylation *(in A)* and protein radical adduct of DMPO *(in B)* measured by immunomicroscopic fluororescence using anti-GSH or anti-DMPO monoclonal antibody.

Fig. S10. Amino acid sequence coverage of the precursor of the 75 kDa subunit from the alkylated control complex I as analyzed by nano-LC/MS/MS. The regions labeled with *italic* bold and represent the amino acid

residues identified with LC/MS/MS under the non-reduced conditions in the absence of β-ME. The cysteinyl residues involved in disulfide bond are detected between C_{554}, *and* C_{564}. *Iodoacetamide alkylation was detected at all cysteine residues except* C_{64} *and* C_{710} *which were not observed by MS/MS.* The region labeled with a dotted underline is the N-terminal extension (aa 1-23), which acts as an import sequence and does not exist in the mature protein.

Supplemental Fig. S1

A *Complex I (NQR)*

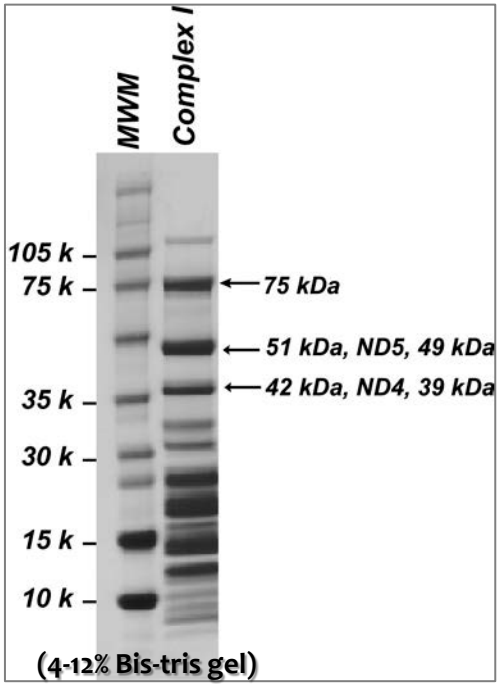

B

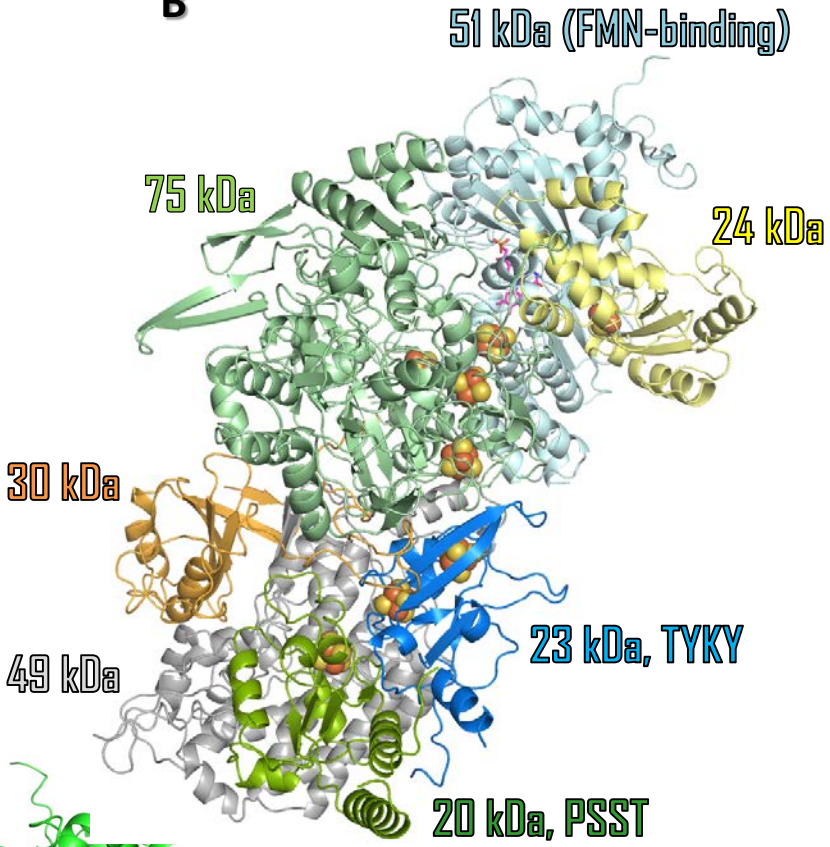

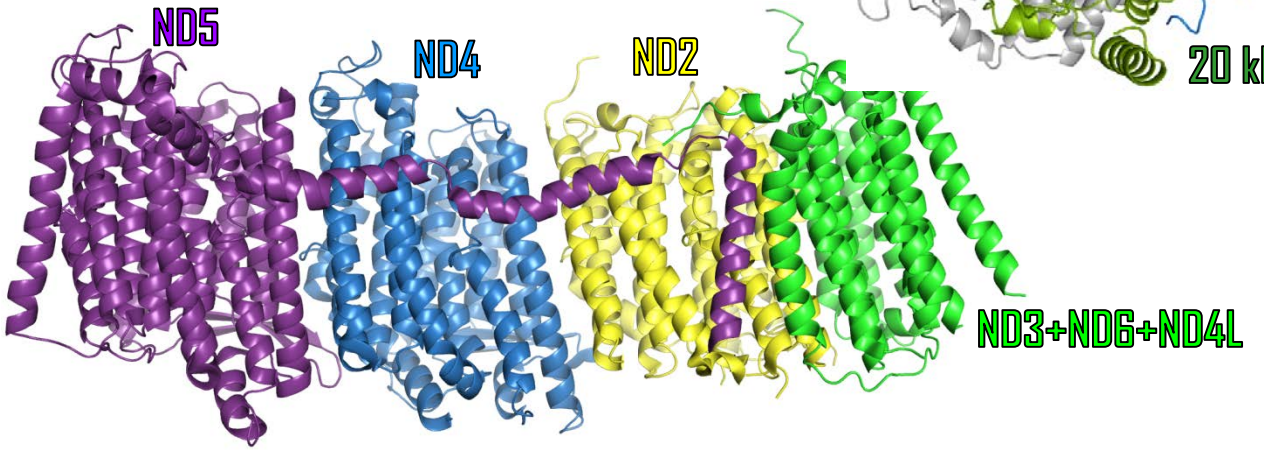

Supplemental Fig. S2

```
  1 MLRIPVRKAL VGLSKSSKGC VRTTATAASN LIEVFVDGQS VMVEPGTTVL
 51 QACEKVGMQI PRFCYHERLS VAGNCRMCLV EIEKAPKVVA ACAMPVMKGW
101 NILTNSEKTK KAREGVMEFL LANHPLDCPI CDQGGECDLQ DQSMMFGSDR
151 SRFLEGKRAV EDKNIGPLVK TIMTRCIQCT RCIRFASEIA GVDDLGTTGR
201 GNDMQVGTYI EKMFMSELSG NIIDICPVGA LTSKPYAFTA RPWETRKTES
251 IDVMDAVGSN IVVSTRTGEV MRILPRMHED INEEWISDKT RFAYDGLKRQ
301 RLTEPMVRNE KGLLTHTTWE DALSRVAGML QSFQGNDVAA IAGGLVDAEA
351 LIALKDLLNR VDSDTLCTEE VFPTAGAGTD LRSNYLLNTT IAGVEEADVV
401 LLVGTNPRFE APLFNARIRK SWLHNDLKVA LIGSPVDLTY RYDHLGDSPK
451 ILQDIASGSH PFSQVLQEAK KPMVILGSSA LQRNDGAAIL AAVSNIAQKI
501 RTSSGVTGDW KVMNILHRIA SQVAALDLGY KPGVEAIQKN PPKMLFLLGA
551 DGGCITRQDL PKDCFIVYQG HHGDVGAPIA DVILPGAAYT EKSATYVNTE
601 GRAQQTKVAV TPPGLAREDW KIIRALSEIA GMTLPYDTLD QVRNRLEEVS
651 PNLVRYDDVE GANYFQQASE LSKLVNQQLL ADPLVPPQLT IKDFYMTDSI
701 SRASQTMAKC VKAVTEGAHA VEEPSIC
```

Sequence coverage=511/704=72.58%

Supplemental Fig. S3a

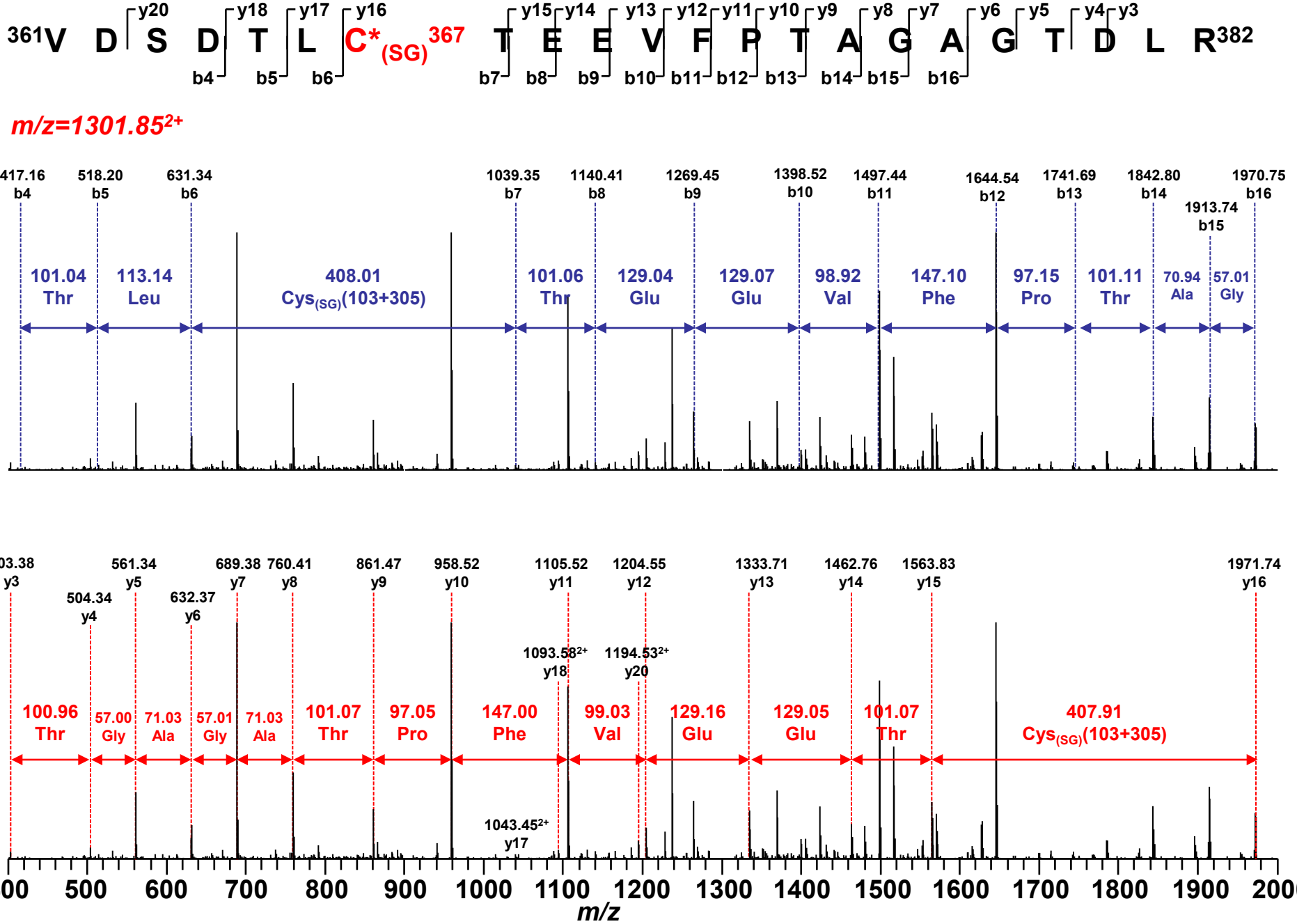

Supplemental Fig. S3b

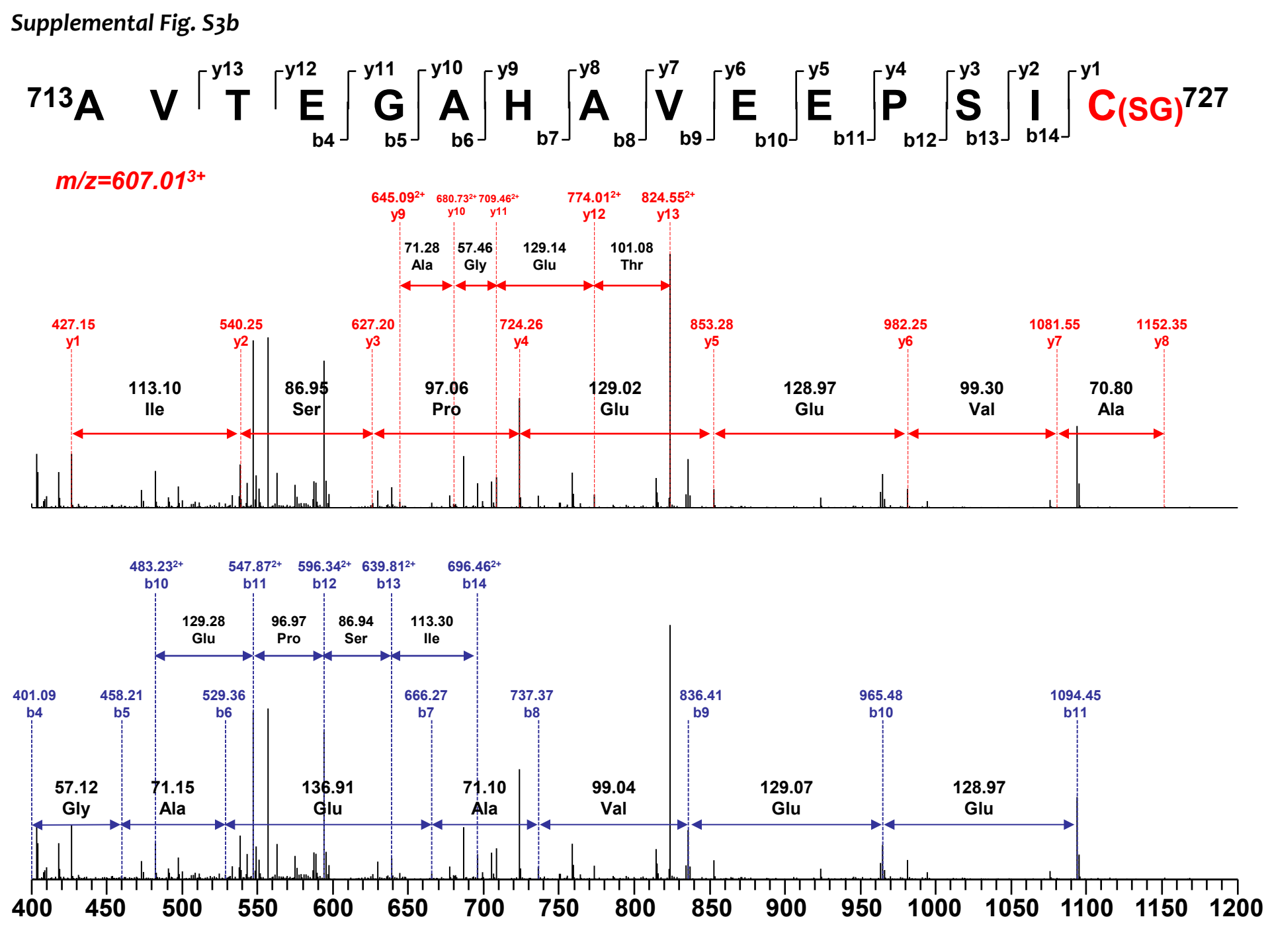

Supplemental Fig. S4

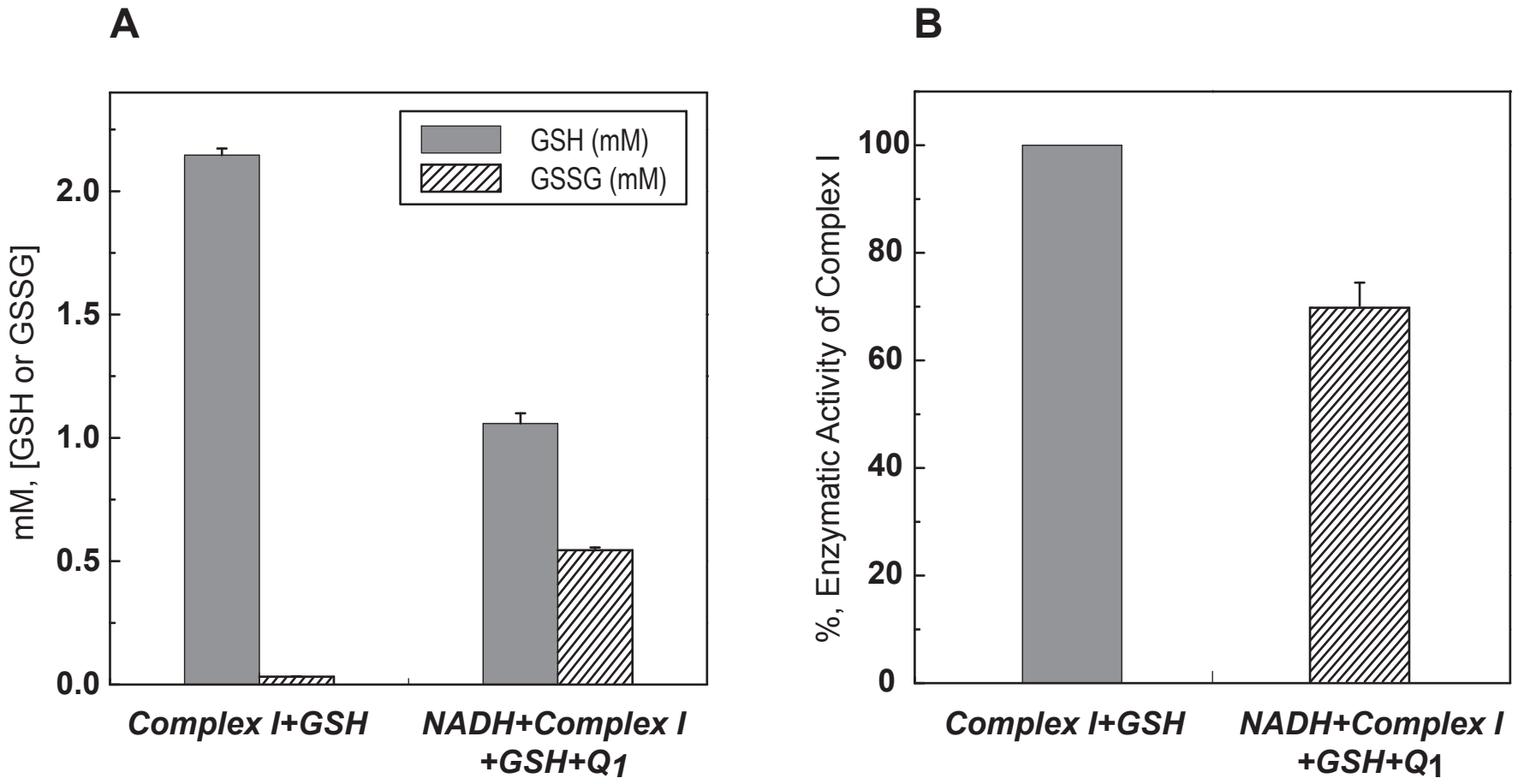

Supplemental Fig. S5

```
   1 MLRIPVRKAL VGLSKSSKGC VRTTATAASN LIEVFVDGQS VMVEPGTTVL
  51 QACEKVGMQI PRFCYHERLS VAGNCRMCLV EIEKAPKVVA ACAMPVMKGW
 101 NILTNSEKTK KAREGVMEFL LANHPLDCPI CDQGGECDLQ DQSMMFGSDR
 151 SRFLEGKRAV EDKNIGPLVK TIMTRCIQCT RCIRFASEIA GVDDLGTTGR
 201 GNDMQVGTYI EKMFMSELSG NIIDICPVGA LTSKPYAFTA RPWETRKTES
 251 IDVMDAVGSN IVVSTRTGEV MRILPRMHED INEEWISDKT RFAYDGLKRQ
 301 RLTEPMVRNE KGLLTHTTWE DALSRVAGML QSFQGNDVAA IAGGLVDAEA
 351 LIALKDLLNR VDSDTLCTEE VFPTAGAGTD LRSNYLLNTT IAGVEEADVV
 401 LLVGTNPRFE APLFNARIRK SWLHNDLKVA LIGSPVDLTY RYDHLGDSPK
 451 ILQDIASGSH PFSQVLQEAK KPMVILGSSA LQRNDGAAIL AAVSNIAQKI
 501 RTSSGVTGDW KVMNILHRIA SQVAALDLGY KPGVEAIQKN PPKMLFLLGA
 551 DGGCITRQDL PKDCFIVYQG HHGDVGAPIA DVILPGAAYT EKSATYVNTE
 601 GRAQQTKVAV TPPGLAREDW KIIRALSEIA GMTLPYDTLD QVRNRLEEVS
 651 PNLVRYDDVE GANYFQQASE LSKLVNQQLL ADPLVPPQLT IKDFYMTDSI
 701 SRASQTMAKC VKAVTEGAHA VEEPSIC
Sequence coverage=679/704 =96.44%
```

Supplemental Fig. S6

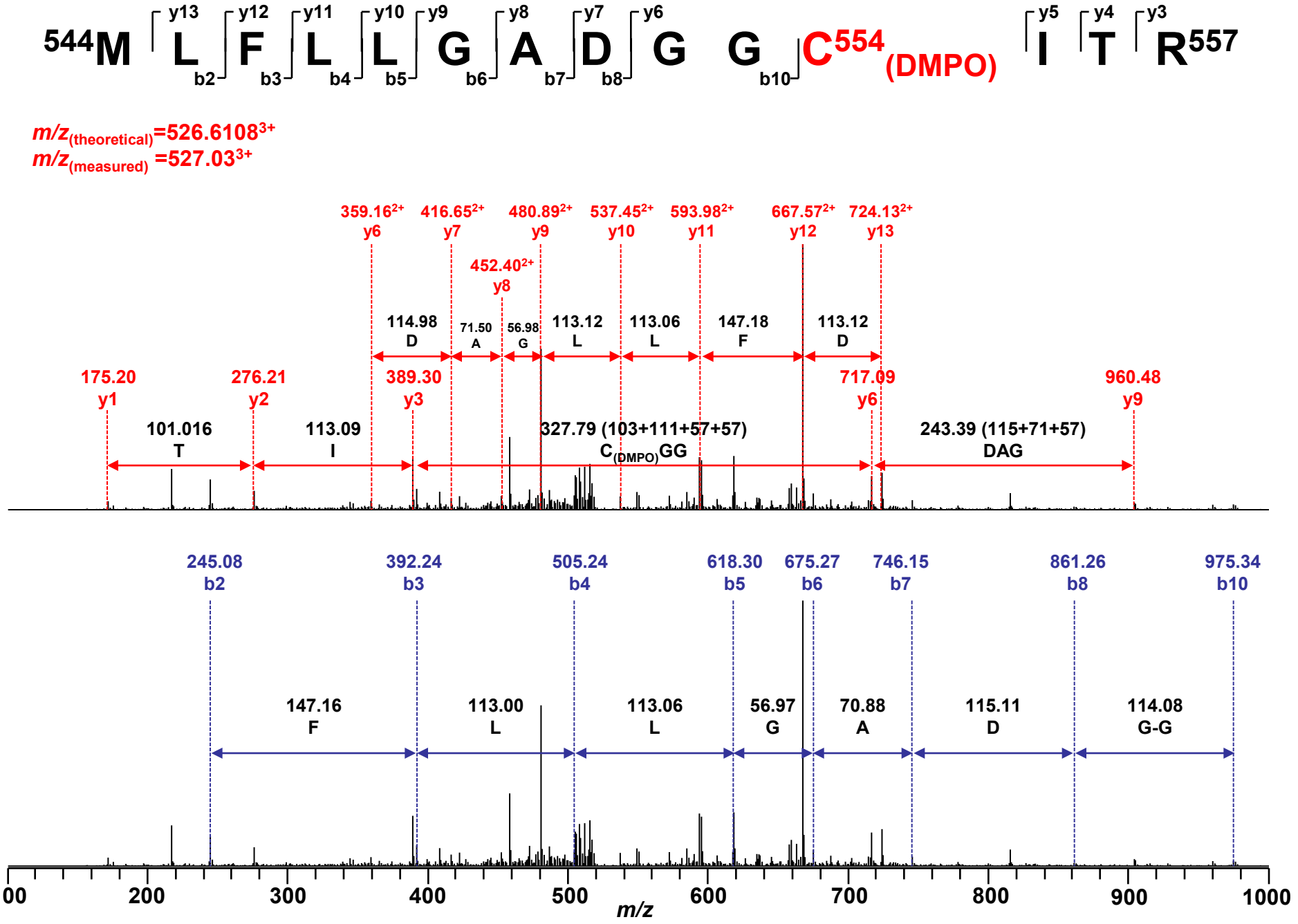

Supplemental Fig. S7a

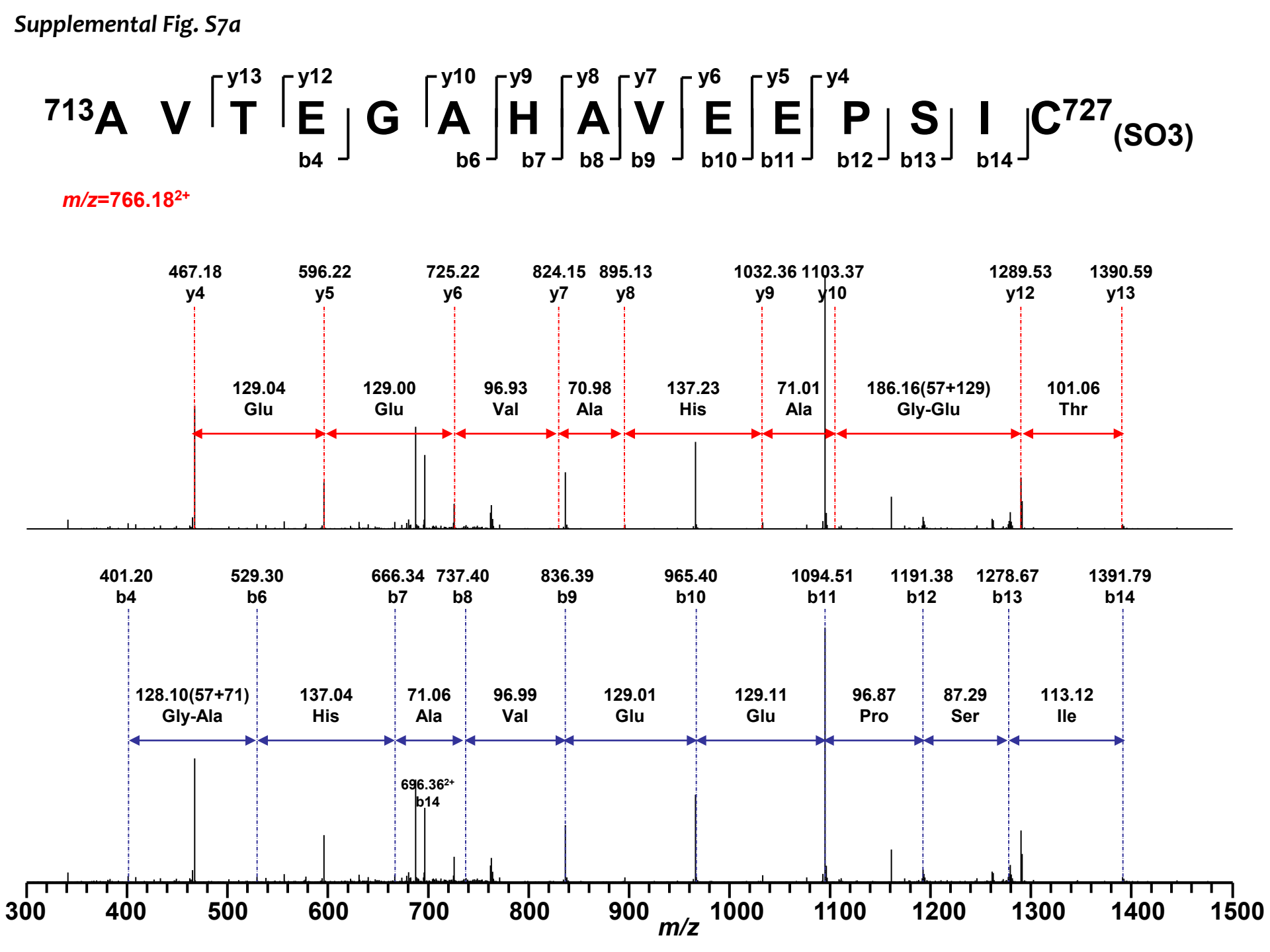

Supplemental Fig. S7b

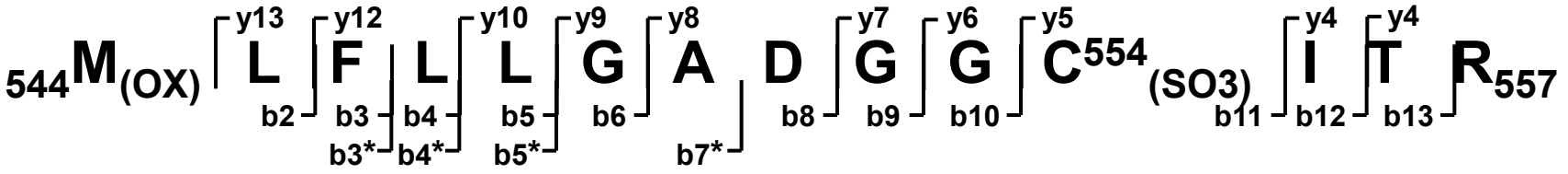

m/z=780.83^{2+}

bn*=bn–CH_4SO

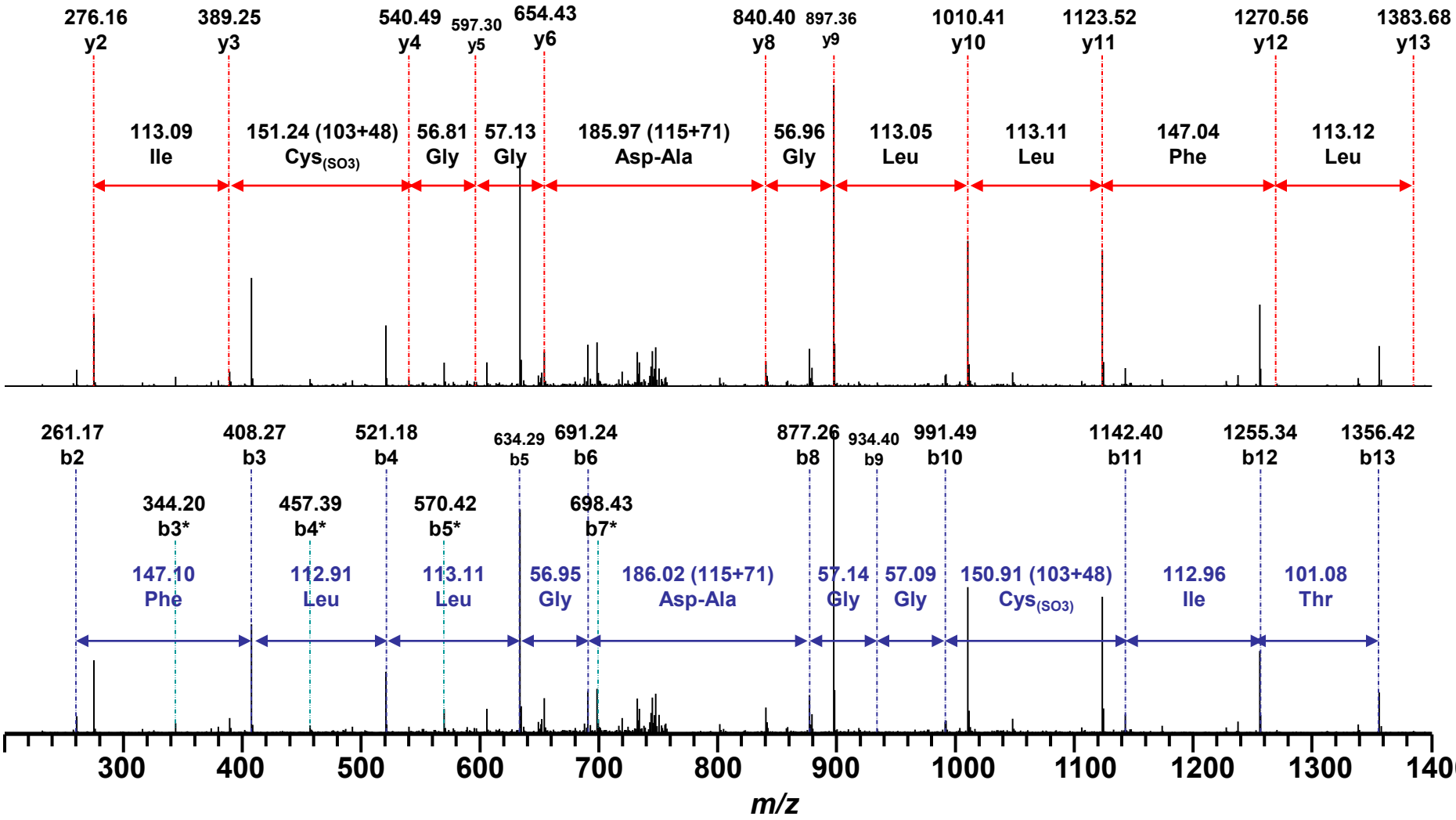

Supplemental Fig. 8S

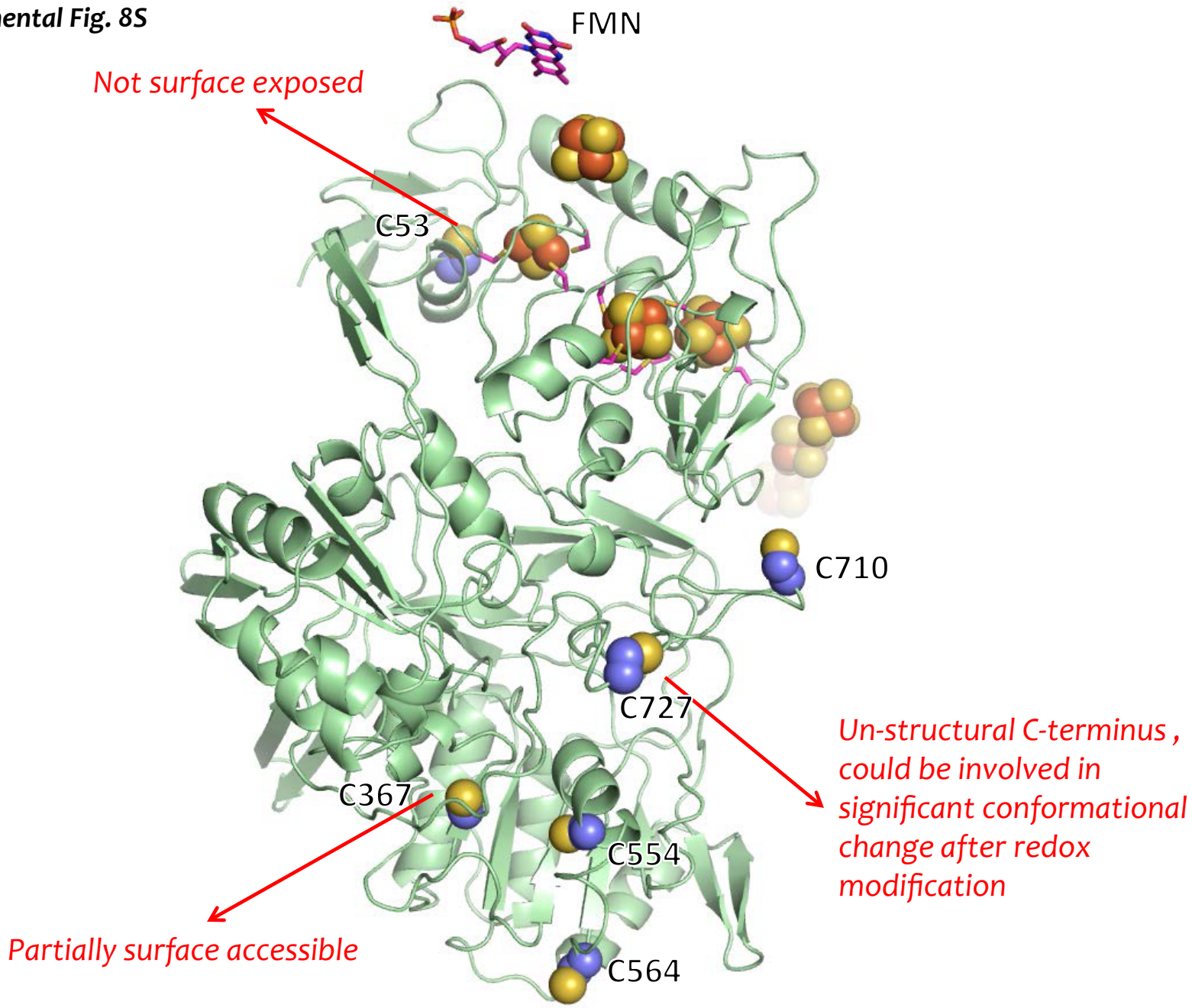

Supplemental Fig. S9

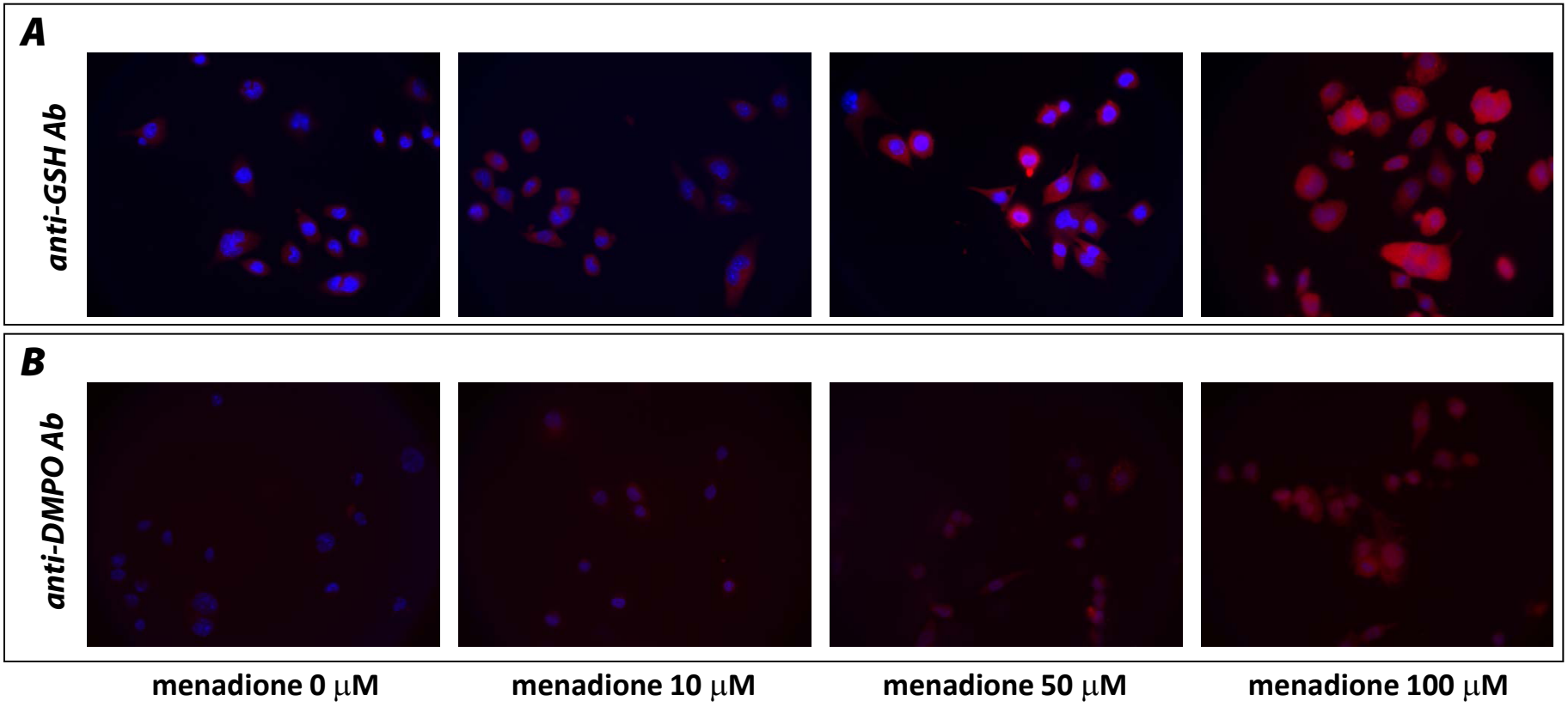

Red: Alexa Fluor 594 -conjugated goat anti-mouse IgG
Blue: DAPI staining of nuclear

Supplementary Fig. S10

```
   1 MLRIPVRKAL VGLSKSSKGC VRTTATAASN LIEVFVDGQS VMVEPGTTVL
  51 QACEKVGMQI PRFCYHERLS VAGNCRMCLV EIEKAPKVVA ACAMPVMKGW
 101 NILTNSEKTK KAREGVMEFL LANHPLDCPI CDQGGECDLQ DQSMMFGSDR
 151 SRFLEGKRAV EDKNIGPLVK TIMTRCIQCT RCIRFASEIA GVDDLGTTGR
 201 GNDMQVGTYI EKMFMSELSG NIIDICPVGA LTSKPYAFTA RPWETRKTES
 251 IDVMDAVGSN IVVSTRTGEV MRILPRMHED INEEWISDKT RFAYDGLKRQ
 301 RLTEPMVRNE KGLLTHTTWE DALSRVAGML QSFQGNDVAA IAGGLVDAEA
 351 LIALKDLLNR VDSDTLCTEE VFPTAGAGTD LRSNYLLNTT IAGVEEADVV
 401 LLVGTNPRFE APLFNARIRK SWLHNDLKVA LIGSPVDLTY RYDHLGDSPK
 451 ILQDIASGSH PFSQVLQEAK KPMVILGSSA LQRNDGAAIL AAVSNIAQKI
 501 RTSSGVTGDW KVMNILHRIA SQVAALDLGY KPGVEAIQKN PPKMLFLLGA
 551 DGGCITRQDL PKDCFIVYQG HHGDVGAPIA DVILPGAAYT EKSATYVNTE
 601 GRAQQTKVAV TPPGLAREDW KIIRALSEIA GMTLPYDTLD QVRNRLEEVS
 651 PNLVRYDDVE GANYFQQASE LSKLVNQQLL ADPLVPPQLT IKDFYMTDSI
 701 SRASQTMAKC VKAVTEGAHA VEEPSIC
```

Sequence coverage = 634/704=90.05%

Supplementary Table

A. Detailed MS/MS map of $_{544}M_{(OX)}LFLLGADGGC_{(SO_2)}{}^{554}ITR_{557}$

Δm between y-n and yn-1	Fragment Ion	Measured m/z	Sequence	Measured m/z	Fragment Ion	Δm between bn and bn-1
			$Met_{(OX)}$			
			Leu	261.02	$\mathbf{b_2}$	
146.76	$\mathbf{y_{12}}$	1254.59	Phe	408.15	$\mathbf{b_3}$	147.13
113.36	$\mathbf{y_{11}}$	1107.83	Leu	521.28	$\mathbf{b_4}$	113.13
113.14	$\mathbf{y_{10}}$	994.47	Leu	634.27	$\mathbf{b_5}$	112.99
56.81	$\mathbf{y_9}$	881.33	Gly	691.39	$\mathbf{b_6}$	57.12
186.2 (115+71)	$\mathbf{y_8}$	824.52	Ala			
			Asp	877.41	$\mathbf{b_8}$	186.02 (71+115)
56.88	$\mathbf{y_6}$	638.32	Gly	934.33	$\mathbf{b_9}$	56.92
57.17	$\mathbf{y_5}$	581.44	Gly	991.42	$\mathbf{b_{10}}$	57.09
135 (103+32)	**y_4**	**524.27**	**$Cys_{(SO_2)}$**	**1126.41**	**b_{11}**	**134.99 (103+32)**
113.19	$\mathbf{y_3}$	389.27	Ile	1239.46	$\mathbf{b_{12}}$	113.05
	$\mathbf{y_2}$	276.08	Thr	1340.80	$\mathbf{b_{13}}$	
			Arg			

B. Detailed MS/MS map of $^{713}AVTEGAHAVEEPSIC_{(SO_2)}{}^{727}$

Δm between yn and yn-1	Fragment Ion	Measured m/z	Sequence	Measured m/z	Fragment Ion	Δm between bn and bn-1
			Ala			
			Val			
99.82	$\mathbf{y_{13}}$	687.50^{+2}	Thr	272.26	$\mathbf{b_3}$	
128.98	$\mathbf{y_{12}}$	637.59^{+2}	Glu	401.22	$\mathbf{b_4}$	128.96
57.78	$\mathbf{y_{11}}$	573.13^{+2}	Gly	458.61	$\mathbf{b_5}$	57.39
71.11	$\mathbf{y_{10}}$	1087.48	Ala	529.29	$\mathbf{b_6}$	70.68
137.08	$\mathbf{y_9}$	1016.37	His	666.41	$\mathbf{b_7}$	137.12
70.75	$\mathbf{y_8}$	879.29	Ala			
99.23	$\mathbf{y_7}$	808.54	Val	836.44	$\mathbf{b_9}$	170.03 (71+99)
129.07	$\mathbf{y_6}$	709.31	Glu	965.40	$\mathbf{b_{10}}$	128.96
129.01	$\mathbf{y_5}$	580.24	Glu	1094.48	$\mathbf{b_{11}}$	129.08
	$\mathbf{y_4}$	451.23	Pro	1191.53	$\mathbf{b_{12}}$	97.05
			Ser	1278.58	$\mathbf{b_{13}}$	113.28
			Ile	696.43^{+2}	$\mathbf{b_{14}}$	
			$Cys_{(SO_2)}$			